Reconstruction of Inundation and Greenhouse Gas Emissions from Siberian Wetlands over the Last Half-Century

Theodore J. Bohn[1], Erika Podest[2], Ronny Schroeder[2], Kyle C. McDonald[2], Chun-mei Chiu[3], Laura C. Bowling[3], Mikhail Glagolev[4], and Dennis P. Lettenmaier[1]

[1]University of Washington, Seattle, Washington, USA; [3]JPL-NASA, Pasadena, California, USA; [3]Purdue University, West Lafayette, Indiana, USA; [4]Moscow State University, Moscow, Russia

AGU Fall Meeting, San Francisco, CA, December 17, 2009

Abstract

Changes in greenhouse gas emissions such as methane (CH4) and carbon dioxide (CO2) from high-latitude wetlands in a warming climate may have important implications for projections of global warming, due to the large amounts of carbon stored in high-latitude soils and the high greenhouse warming potential of methane. As much as 1/3 of global natural methane emissions come from high latitudes. Efforts to monitor high-latitude greenhouse gas emissions are hampered by the sparseness of in situ data at high latitudes, especially in Northern Eurasia. While biogeochemical modeling can provide estimates of greenhouse gas emissions in such areas, the lack of in situ measurements also makes it difficult to constrain these models. Fortunately, emissions of greenhouse gases, especially methane, are sensitive to hydrologic variables such as inundation that now can be observed via passive microwave and synthetic aperture radar remote sensors. Here we apply a combination of large-scale hydrologic/biogeochemical models and remote sensing observations across the West Siberian lowlands to estimate soil moisture, inundation, and greenhouse gas fluxes. Our modeling framework consists of the Variable Infiltration Capacity macroscale hydrological model (VIC), extended to include carbon cycling and coupled to a methane emissions model. In particular, our modeling framework includes a parameterization of the spatial distribution of soil moisture, which allows us to compare our simulated emissions to both large-scale remote sensing observations and point-scale in-situ observations. We have calibrated this framework using observed streamflow, inundation products derived from PALSAR and AMSR-E, and in situ water table and greenhouse gas emissions observations. Using the calibrated model, we examine the interannual variability of simulated inundation and greenhouse gas emissions across W. Siberia for the period 1948-2007.

1. Modeling Approach

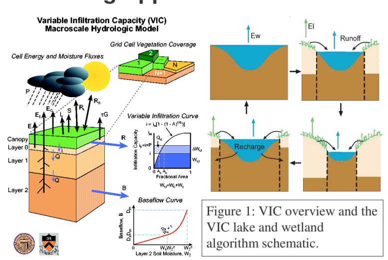

Figure 1: VIC overview and the VIC lake and wetland algorithm schematic.

Land Surface Hydrology Model

- Variable Infiltration Capacity (VIC) Model (Liang et al. 1994)
- Water and energy balance closure
- Macroscale: grid cells range from 10 to 100 km
- Statistical parameterizations of sub-grid variability in soil moisture, land cover
- Lake/wetland model (Bowling, 2002) handles changes in lake extent
- Grid cell average water table computed as sum of total column soil moisture deficit
- Extended to handle carbon cycling with Farquhar photosynthesis, plant respiration, and NPP from BETHY (Knorr, 2000)

Sub-grid Variability of Water Table and Inundation

- Uses topographic wetness index formulation from TOPMODEL (Beven and Kirkby, 1979)
- Relates local water table position to local topography and the average water table depth of the region

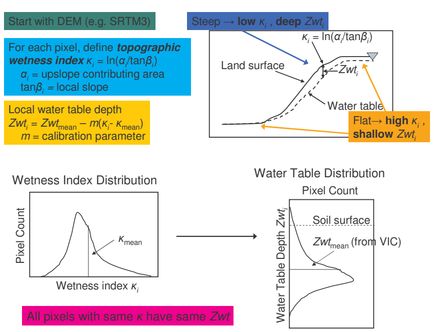

Methane Model

- Walter and Heimann (2000) with modifications described in Walter et al (2001a)
- soil methane production, and transport of methane by diffusion, ebullition, and through plants modeled explicitly
- methane production occurs in the anoxic soil from the bottom of the soil column to the water table
- methane production rate controlled by soil temperature and NPP (both from VIC)
- methane oxidation also taken into account

Model Framework

- VIC hydrologic model driven by (1) gridded meteorological forcings and (2) wetness index distribution from SRTM3 and GTOPO30 DEMs
- VIC produces daily Zwt with modifications
- VIC produces daily Zwt(x,y), SoilT, and NPP
- Distributed Zwt(x,y,t), SoilT, and NPP drive methane and soil respiration models, which produce CH4(x,y,t) and CO2(x,y,t)

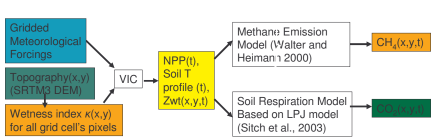

2. Study Domain

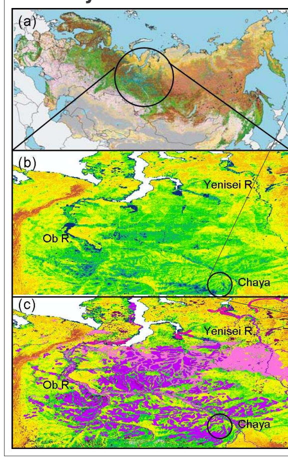

Fig. 1. Our current study domain, circled in panel (a), is the West Siberian Lowlands, home to a large portion of the world's wetlands. Panel (b) shows the topographic wetness index across this domain, derived from SRTM3 and GTOPO30 DEMs. Red = low wetness index, blue = high wetness index. Panel (c) overlays the wetland delineation of Lehner and Doll (2004). It can be seen that the spatial distribution of wetlands correlates strongly with high values of wetness index.

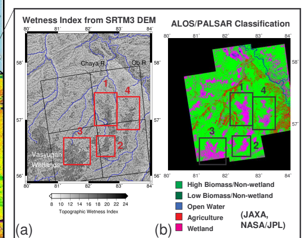

Fig. 2. Focus area: Chaya/Bakchar/Iksa watershed. We are running our modeling framework at a resolution of 100km (EASE grid equal-area polar projection) (grid cells outlined in panel (a)). Topography is supplied by the SRTM 30m UTM DEM. For comparison with simulations, and to calibrating the modeling framework, we have classified 12.5m UTM PALSAR imagery from the region (panel (b)), acquired in the summers of 2006-07. Classes of particular interest are: open water and saturated/inundated land (with emergent vegetation) (listed as "wetland" in the legend in panel (b)). To calibrate the water table parameterization, we have selected 4 regions of interest (ROIs), shown as numbered boxes in panels (a) and (b).

3. Model Calibration

We are calibrating the modeling framework using a combination of *in situ* and remotely-sensed observations:

1. Gauged streamflows in sub-basins covering 70% of the region, 1950-1970. These help constrain the depth of the simulated soil column, its drainage properties, and the relationship between topographic wetness index and water table depth.

2. Remotely-sensed observations of inundation, derived from Landsat, AMSR-E, and PALSAR imagery, 1970s through 2007. These help constrain lake drainage and the relationship between topographic wetness index and water table depth.

3. In situ measurements of CH4 and CO2 emissions at a small number of locations in the domain. These help constrain carbon cycle parameters but due to their scarcity, we will need to explore the responses over a range of plausible parameter values.

Figure 3. Simulated and observed inundation from ROIs in Figure 2.

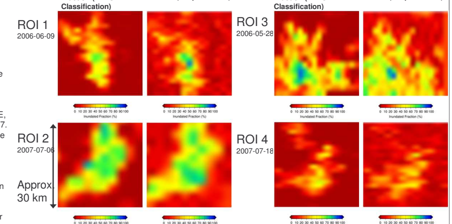

For each of the ROIs in fig. 2, we aggregated the remote sensing classifications up to 2700m resolution, computing the fraction of inundated 12.5m pixels in each 2700m "cell". Examples of observed inundation at each of the ROIs are shown in the first and third columns of fig. 3, along with acquisition dates.

Before analyzing topography, we first smoothed the DEM with a cutoff wavelength of 2100 m, to reduce noise in the DEM caused by its coarse (1 m) vertical resolution and the effects of scattered tree canopies on the DEM. Then we computed wetness index values at all 30 m pixels of the smoothed DEM.

For each ROI, we aggregated to 2700 m resolution, computing the fraction of 30 m DEM pixels having wetness index κ_i > threshold κ_t within each 2700 m cell, for a range of threshold k_t values. For each κ_t value, we evaluated the bias: mean(fraction >= κ_t) - mean(fraction_inundated). We then selected the κ_t value for which bias was smallest as the "best" estimate for that ROI and date. Maps of fraction above threshold at each of the ROIs on the same dates as the observations are shown in the second and fourth columns of fig. 3. The strong correspondence between the spatial distributions of simulated and observed inundation is evident.

6. Conclusions and Future Work

Conclusions

- The TOPMODEL approximation gives a good fit to the spatial distribution of wetlands, offering a relatively inexpensive method for increasing the accuracy of methane emissions estimates from global large-scale models
- One benefit of the distributed water table parameterization is that it allows us to convert simulated water table depth into inundated extent, which can be observed by satellite
- Predicted methane emissions and greenhouse warming potential are very sensitive to how the water table varies across the landscape; models using uniform water table likely overestimate the response of wetland methane emissions
- Combining remote sensing data and models allows us to better understand the behavior of wetlands across vast, relatively inaccessible areas
- The ability to validate with remote sensing offers possibility of data assimilation schemes to enhance real-time monitoring

Future Work

- Explore the effects of errors in the TOPMODEL parameterization, and uncertainty in model parameter values, on simulated inundated extent and CH4 emissions
- Explore the statistical relationships among T, P, Zwt, inundation, and CH4 emissions over the period 1948-2007, including trend analysis and persistence
- Explore spatial variation in sensitivity of methane emissions to climate factors and parameter uncertainty, and identify areas where future observations might be most beneficial
- Extend analysis to all of West Siberian Lowlands

* References available upon request

4. Interannual Variability

Using the parameters described in section 3, we have run simulations for the Chaya/Bakchar/Iksha basin for the period 1948-2007. Meteorologic inputs were generated from gridded observations according to the procedure of Adam et al. (2007). The resulting time series of annual precipitation, average 10 cm soil temperature, average water table position, average inundated fraction, and average methane emissions are shown in fig. 4 a-e.

It can be seen that annual methane emissions (fig. 4.e.) respond to both soil temperature (fig. 4.b.) and basin-wide water table position (fig. 4.c.) (or inundated fraction (fig. 4.d.), which is non-linearly dependent on water table position). We have not yet performed statistical analyses on the data. However, we can identify several areas that warrant examination:

1. There appears to be a positive trend in soil temperature since the late 1960s (fig 4.b.). This trend also appears to be present in the methane emissions. We would expect that trends in summer temperatures would directly affect methane emissions via changes in metabolic rates, and indirectly via changes in water table depth (through evaporation rates). Meanwhile, trends in winter temperatures would affect snow pack accumulation rates and the timing and strength of spring snow melt. A trend analysis of not only annual average values but also of seasonal values could help us understand which climate factors exert the most influence on methane emissions rates.

2. Basin-average water table position appears to exhibit some correlation with annual precipitation, along with some degree of interannual persistence, which can be expected in reservoirs with residence times longer than one year. It would be interesting to examine the autocorrelation of water table position and methane emissions, for a variety of possible model soil parameterizations, to assess their potential effects on interannual variability of methane emissions.

Three years, 1980, 1994, and 2002 have been identified in fig. 4. for discussion in section 5, below. 1980 represents an "average" year, with temperature and water table in the middle of their ranges. 2002 is a "warm, wet" year with extremely high water table and warmer than average temperature. 1994 is a "warm, dry" year, with high temperature but slightly lower than average water table.

Fig. 4. Annual time series of relevant variables, Chaya basin, 1948-2007

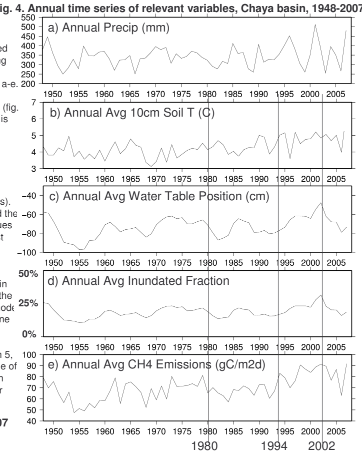

Fig. 5. Annual time series of GWP of carbon fluxes, Chaya basin, 1948-2007

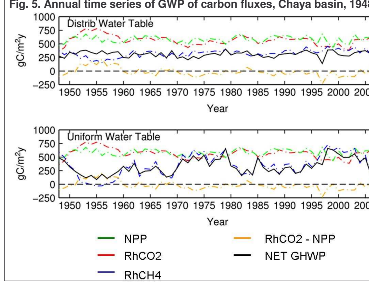

Figure 5 shows the effects of using a distributed water table versus the more traditional approach of using a uniform water table across each grid cell. The greenhouse warming potential (GWP) of simulated annual carbon fluxes from the Chaya basin, 1948-2007, for the distributed water table (upper panel) and uniform water table (lower panel). For methane (RhCH4; blue), GWP = 23 gC/gCH4 for a 100-year time horizon. On the other hand, the GWP of net primary productivity (NPP; green) and aerobic soil respiration (RhCH4; blue) are 1. Thus, while methane comprises a small portion of the annual carbon budget, it plays a significant role in the annual GWP of the system. In both cases, NPP and RhCO2 tend to be similar in magnitude on an annual basis, so that their difference (RhC02-NPP; orange) tends to be smaller than the GWP of methane emissions. Therefore, methane emissions dominate the system's annual GWP.

Methane emissions are strongly sensitive to water table depth, in a non-linear way. The uniform water table scheme (lower panel) yields a much more dramatic ("flashier") methane emissions response, because water table depth across the entire grid cell rises and falls in unison. The distributed water table case (upper panel) has a more muted response, due to the smooth increase/decrease in saturated area across the grid cell. This has important implications for any inferred trends in both methane emissions and GWP in response to trends in climate; models using the traditional uniform water table scheme may therefore overestimate trends in future GWP.

5. Spatial Variability of Inundation and Methane Emissions

Fig. 6. Simulated Inundated Fraction and CH4 Emissions for Selected Years

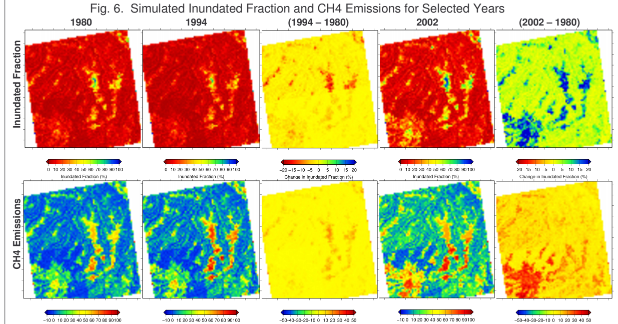

1994: A Warm, Dry Year

Inundation decreased, especially in the north of the basin, due to increased evaporation.

CH4 emissions increased via increased metabolic rates in response to higher temperatures, despite the reduction in inundated area. An exception to this is the lower left grid cell, which was so dry to begin with that the increase in metabolic rates did not help.

Responses of CH4 Emissions to T and P

1980: An "Average" Year

Inundation and CH4 emissions are strongest in bogs, as we would expect.

Lower-left 100km grid cell is drier than the others, and has accordingly lower CH4 emissions.

2002: A Warm, Wet Year

Inundation increases occurred consistently throughout the bogs, in all grid cells.

Increases in CH4 emissions also occurred throughout the bogs. However, lower-left grid cell emissions increased more than the others,

Take-away point: most variation of both inundation and CH4 emissions occurs in the wettest areas, i.e. bogs, in part because inundation is non-linear function of water table.